

**Olasunkanmi A. J. Adegoke, Stéphanie Chevalier, José A. Morais, Réjeanne Gougeon, Scot R. Kimball, Leonard S. Jefferson, Simon S. Wing and Errol B. Marliss**

*Am J Physiol Endocrinol Metab* 296:105-113, 2009. First published Oct 28, 2008;  
doi:10.1152/ajpendo.90752.2008

**You might find this additional information useful...**

---

This article cites 48 articles, 27 of which you can access free at:

<http://ajpendo.physiology.org/cgi/content/full/296/1/E105#BIBL>

Updated information and services including high-resolution figures, can be found at:

<http://ajpendo.physiology.org/cgi/content/full/296/1/E105>

Additional material and information about *AJP - Endocrinology and Metabolism* can be found at:

<http://www.the-aps.org/publications/ajpendo>

---

This information is current as of February 9, 2010 .

## Fed-state clamp stimulates cellular mechanisms of muscle protein anabolism and modulates glucose disposal in normal men

Olasunkanmi A. J. Adegoke,<sup>1,2</sup> Stéphanie Chevalier,<sup>2,3</sup> José A. Morais,<sup>2,3</sup> Réjeanne Gougeon,<sup>2,3</sup> Scot R. Kimball,<sup>4</sup> Leonard S. Jefferson,<sup>4</sup> Simon S. Wing,<sup>3,5</sup> and Errol B. Marliss<sup>2,3</sup>

<sup>1</sup>School of Kinesiology and Health Science, York University, Toronto, Ontario; and <sup>2</sup>McGill Nutrition and Food Science Centre, McGill University and <sup>3</sup>Division of Endocrinology and Metabolism, Department of Medicine, McGill University Health Centre/Royal Victoria Hospital, Montreal, Quebec, Canada; <sup>4</sup>Department of Cellular and Molecular Physiology, Pennsylvania State University College of Medicine, Hershey, Pennsylvania; and <sup>5</sup>Polypeptide Hormone Laboratory, McGill University, Montreal, Quebec, Canada

Submitted 5 September 2008; accepted in final form 24 October 2008

**Adegoke OA, Chevalier S, Morais JA, Gougeon R, Kimball SR, Jefferson LS, Wing SS, Marliss EB.** Fed-state clamp stimulates cellular mechanisms of muscle protein anabolism and modulates glucose disposal in normal men. *Am J Physiol Endocrinol Metab* 296: E105–E113, 2009. First published October 28, 2008; doi:10.1152/ajpendo.90752.2008.—Since maximum anabolism occurs postprandially, we developed a simulated fed state with clamped hyperinsulinemia, physiological hyperglycemia, and hyperaminoacidemia (Hyper-3) and explored muscle cellular mechanisms. Whole body [<sup>1-<sup>13</sup>C</sup>]leucine and [<sup>3-<sup>3</sup>H</sup>]glucose kinetics in healthy men were compared between hyperinsulinemic, euglycemic, isoaminoacidemic (Hyper-1, *n* = 10) and Hyper-3 (*n* = 9) clamps. In Hyper-3 vs. Hyper-1, nonoxidative leucine *R*<sub>d</sub> [rate of disappearance (synthesis)] was stimulated more (45 ± 4 vs. 24 ± 4 μmol/min, *P* < 0.01) and endogenous *R*<sub>a</sub> [rate of appearance (breakdown)] was inhibited similarly; hence net balance increased more (86 ± 6 vs. 49 ± 2 μmol/min, *P* < 0.001). Glucose *R*<sub>d</sub> was similar; thus Hyper-3 metabolic clearance rate (331 ± 23 vs. 557 ± 41 ml/min, *P* < 0.0005) and *R*<sub>d</sub>/insulin (M, 0.65 ± 0.10 vs. 1.25 ± 0.10 mg·min<sup>-1</sup>·pmol<sup>-1</sup>·l, *P* < 0.001) were less, despite higher insulin (798 ± 74 vs. 450 ± 24 pmol/l, *P* < 0.005). In vastus lateralis muscle biopsies, phosphorylation of Akt (*P* = 0.025), mammalian target of rapamycin (mTOR), ribosomal protein S6 kinase (p70<sup>S6K1</sup>; *P* = 0.008), S6 (*P* = 0.049), and 4E-binding protein 1 (4E-BP1; *P* = 0.001) increased. With decreased eukaryotic initiation factor-4E (eIF4E)·4E-BP1 complex (*P* = 0.01), these are consistent with increased mTOR complex 1 (mTORC1) signaling and translation initiation of protein synthesis. Although mRNA expression of ubiquitin, MAFbx 1, and MuRF-1 was unchanged, total ubiquitinated proteins decreased 20% (*P* < 0.01), consistent with proteolysis suppression. The Hyper-3 clamp increases whole body protein synthesis, net anabolism, and muscle protein translation initiation pathways and decreases protein ubiquitination. The main contribution of hyperaminoacidemia is stimulation of synthesis rather than inhibition of proteolysis, and it attenuates the expected increment of glucose disposal.

translation initiation; ubiquitin pathway; leucine kinetics; glucose turnover; insulin resistance

THE HYPERINSULINEMIC EUGLYCEMIC CLAMP is the “gold standard” for determining *in vivo* insulin sensitivity of glucose metabolism. Although the conventional clamp achieves hyperinsulinemia within the postprandial range, it does not replicate post-meal circulating metabolite concentrations. Indeed, it generates

hypoaminoacidemia by insulin inhibition of protein catabolism, thereby preventing the testing of insulin sensitivity of protein anabolism by decreasing amino acid (AA) availability (6, 38, 46). Since insulin stimulation of protein synthesis and inhibition of proteolysis are unambiguously established *in vitro*, and abnormal protein metabolism occurs in both type 1 (45) and type 2 diabetes (17, 19) we have previously used an hyperinsulinemic, euglycemic, isoaminoacidemic clamp (8) to explore whole body protein turnover. This has established the presence of postabsorptive and clamp insulin resistance of protein metabolism in obesity (10), type 2 diabetes (37), and aging (7) and, additionally, sex differences in clamp responses (9). However, this “Hyper-1” clamp does not replicate postprandial physiology, in which plasma insulin, glucose, and AA concentrations increase and free fatty acids (FFA) decrease. Daily repletion of overnight protein depletion must take place at high rates postprandially. We therefore developed a simulated fed steady-state “Hyper-3” clamp with postprandial levels of insulin, glucose, and AA.

Muscle is a principal contributor to whole body substrate metabolism. Since cellular mechanisms responsible for the above insulin-resistant states have not been defined, we combined end points of whole body kinetics with those of regulation of protein metabolism in muscle biopsies. Nutrients, particularly the AA leucine, and insulin regulate protein synthesis by mediating mRNA translation. Leucine and insulin signaling mechanisms converge at the level of the mammalian target of rapamycin (mTOR) (22, 50). mTOR can exist in two distinct complexes, mTORC1 and 2. Activated mTORC1 stimulates translation initiation by phosphorylating 4E-binding protein 1 (4E-BP1), favoring the dissociation of eukaryotic initiation factor (eIF)4E from the inhibitory eIF4E·4E-BP1 complex and the formation of the translation-promoting eIF4E·eIF4G complex. mTORC1 also promotes translation via the phosphorylation of the serine threonine kinase S6K1 (22, 50). In diabetic rats, insulin-independent stimulation of protein synthesis by leucine occurs (3) via eIF4G phosphorylation and its association with eIF4E, without change in mTORC1 signaling to 4E-BP1 or S6K1 (4). Studies of regulation of these and other pathways during oral feeding in humans are demanding because of non-steady-state circulating hormones and substrates and require extremely complex experimental protocols. Addi-

Address for reprint requests and other correspondence: E. B. Marliss, McGill Nutrition & Food Science Centre, MUHC/Royal Victoria Hospital, 687 Pine Ave. West, H6.61, Montreal, QC H3A 1A1, Canada (e-mail: marliss.errol@muhc.mcgill.ca).

The costs of publication of this article were defrayed in part by the payment of page charges. The article must therefore be hereby marked “advertisement” in accordance with 18 U.S.C. Section 1734 solely to indicate this fact.

tionally, since nonphysiological hyperaminoacidemia has been shown to restrain insulin-mediated glucose uptake in euglycemic clamps (27, 47), quantifying this response in fed steady-state conditions should permit elucidation of whether this observation has physiological/pathophysiological implications.

The ubiquitin system is probably the principal regulator of skeletal muscle proteolysis, although other proteases including calpains and cathepsins are involved (21, 34). Ubiquitin is covalently conjugated to lysine residues of proteins via sequential activities of ubiquitin-activating and -conjugating enzymes and ubiquitin-protein ligases. The resultant polyubiquitinated proteins are degraded by the 26S proteasome. In muscle atrophy, mRNA expression of ubiquitin and the ubiquitin-protein ligases MAFbx/Atrogin 1 and MuRF-1, increases (28) in association with increased rates of proteolysis (29). However, their roles in human daily fasting-feeding cycles have not been ascertained.

Thus we studied whole body protein kinetics combined with muscle biopsies to examine concurrent regulation of steps in protein synthetic and catabolic pathways in the Hyper-3 clamp in healthy men. Whole body results are compared with those from Hyper-1 clamps, results from which have been previously published (8, 9). Partial results have appeared in abstract form (2).

## MATERIALS AND METHODS

**Subjects.** Nineteen lean, healthy young men underwent medical history, physical examination, and laboratory investigation, as detailed previously (8). They were admitted to the Royal Victoria Hospital's Clinical Investigation Unit after giving informed consent. This protocol was approved by the institutional Human Ethics Review Committee. Body composition was assessed by bioelectrical impedance analysis with the RJL-101A Systems (Detroit, MI) instrument. Fat-free mass (FFM) was calculated with a sex-specific formula (16). Subjects (Table 1) received a 7-day 15% protein, isoenergetic diet (based on resting metabolic rate by indirect calorimetry with 1.7 physical activity factor) using a liquid formula (Ensure, Abbott Laboratory, St. Laurent, QC, Canada) with breakfast of 30 g of cereal (All-Bran, Kellogg Canada, Etobicoke, ON, Canada) and 200 ml of 2% milk (18).

**Hyperinsulinemic, hyperglycemic, hyperaminoacidemic clamp protocol.** The Hyper-3 clamp is a modification of our Hyper-1 protocol (8). The postprandial target glucose of 8 mmol/l and branched-chain amino acids (BCAA) of 700  $\mu$ mol/l were established from peak responses of seven similar subjects after a 714-kcal, 108 g carbohy-

drate, 30 g protein meal (data from prior study, not shown). At 0800, a catheter was inserted in an antecubital vein for infusions and one was placed in the contralateral hand vein (retrogradely) for blood sampling. The hand was in a heating box at 65–70°C to arterialize the venous blood. Glucose turnover was studied with a primed [22  $\mu$ Ci (814 kBq)] continuous infusion [0.22  $\mu$ Ci/min (8.14 kBq/min)] of [3-<sup>3</sup>H]glucose (PerkinElmer, Boston, MA) begun 180 min before insulin. Concurrently with the tritiated glucose and after 0.1 mg/kg NaH<sup>13</sup>CO<sub>3</sub> (Mass Trace, Woburn, MA) orally, leucine kinetics were studied with a primed (0.5 mg/kg), constant (0.008 mg·kg<sup>-1</sup>·min<sup>-1</sup>) infusion of [<sup>13</sup>C]leucine (Sigma-Aldrich, St. Louis, MO) (33). A primed, constant infusion of human insulin (Humulin R; Eli Lilly, Toronto, ON, Canada) was given at 40 mU·m<sup>-2</sup>·min<sup>-1</sup>, from 0 to 180 min. From 4 min, 20% (wt/vol) potato starch-derived glucose (Avebe, Foxhol, Netherlands) with added [3-<sup>3</sup>H]glucose was infused at rates based on measurements every 5 min (15). BCAA were clamped with a variable infusion of an AA solution (10% TrophAmine; B Braun Medical, Irvine, CA) based on measurements every 5 min. The 10 subjects of the Hyper-1 clamp received the same infusions, but with glycemia maintained at 5.5 mmol/l and BCAA at individual postabsorptive concentrations.

In the Hyper-3 subjects, before and 2 h after start of the clamp, ~100-mg vastus lateralis muscle biopsies were obtained with a Bergstrom needle under sterile precautions and anesthesia (Xylocaine 2%, Astra-Zeneca Canada, Mississauga, ON, Canada), and aliquots were either immediately frozen in liquid nitrogen or homogenized in buffer.

Additional blood samples were collected at baseline and every 10 min for 40 min before clamp and before 120 and 180 min of the clamp (with 30-min sampling otherwise) for substrate, hormone, and isotopic enrichment determinations. Indirect calorimetry was performed for 20 min during these intervals. Glucose turnover was calculated with a method for non-steady-state kinetics (5). Expired air was collected in evacuated tubes (Becton Dickinson Vacutainer Systems, Franklin Lakes, NJ). Leucine kinetics were calculated with plasma  $\alpha$ -keto-isocaproic acid ( $\alpha$ -KIC) as an index of the precursor pool enrichment (reciprocal model) (33). Calculations of [<sup>13</sup>C]leucine oxidation account for the proportion of <sup>13</sup>CO<sub>2</sub> not fully recovered, which varies according to physiological state. We determined the recovery factors previously from [<sup>13</sup>C]bicarbonate studies as being 67.0% for the postabsorptive state and 79.9% for the Hyper-1 protocol (8). A published postprandial state factor of 82.4% was used for Hyper-3 conditions (30). Moreover, dilution of <sup>13</sup>CO<sub>2</sub> natural abundance from infusions was determined in separate experiments for Hyper-1 (8) and in two Hyper-3 subjects, under the same experimental conditions but with no tracers. Dilution factors so determined were 10.1% for Hyper-1 and 13.0% for Hyper-3. Data are presented as units per minute, because the two groups did not differ in body composition. Significance was tested with variables factored for body weight and for FFM, and the outcomes were identical (not shown). Furthermore, responses during the two clamps were shown to be independent of indexes of body composition in this homogeneous group. Data are presented as mean values for the basal period before insulin infusion and for the steady state of the hyperinsulinemic period, including time of biopsy, for the leucine kinetics.

**Assays.** Glucose was measured by glucose oxidase (GM7 Micro-Stat; Analox Instruments USA, Lunenburg, MA); insulin, glucagon and C-peptide by radioimmunoassay (Linco, St. Charles, MO); and glucose specific activity as previously described (7–10, 37). Plasma total BCAA were measured by rapid enzymatic fluorometric assay (8). Plasma AA were determined by HPLC (Beckman Coulter Instruments, Palo Alto, CA). The <sup>13</sup>C enrichment of plasma  $\alpha$ -KIC was analyzed by gas chromatography-mass spectrometry (5988A; Hewlett-Packard, Palo Alto, CA) after derivatization with *N*-methyl-*N*-(*tert*-butyldimethylsilyl)trifluoroacetamide (Regis Technologies, Morton Grove, IL). Expired air was analyzed for <sup>13</sup>CO<sub>2</sub> enrichment

Table 1. Subject characteristics

	Hyper-1	Hyper-3
<i>n</i>	10	9
Age, yr	27 ± 1	29 ± 2
Height, cm	179 ± 2	177 ± 2
Weight, kg	69.1 ± 1.9	66.6 ± 2.2
BMI, kg/m <sup>2</sup>	21.7 ± 0.5	21.2 ± 0.6
FFM, kg	59.4 ± 1.2	58.3 ± 1.7
Percent body fat, %	13.8 ± 1.4	12.4 ± 1.1
Energy intake, MJ/day	11.5 ± 0.4	11.1 ± 0.4
Protein intake, g/day	103 ± 3	101 ± 3
REE, MJ/day	6.8 ± 0.2	6.5 ± 0.3

Values are means ± SE. BMI, body mass index; FFM, fat-free mass; REE, resting energy expenditure. Hyper-1, hyperinsulinemia + euglycemia + isoaminoacidemia; Hyper-3, hyperinsulinemia + hyperglycemia + hyperaminoacidemia.

by isotope ratio mass spectrometry on a Micromass 903D (Vacuum Generators, Winslow, UK).

*Analysis of translation initiation factors and signaling proteins.* Immediately after biopsy, ~30 mg was homogenized in 7 volumes of *buffer A* (in mM: 20 HEPES, 2 EGTA, 50 NaF, 100 KCl, 0.2 EDTA, 50 glycerolphosphate, pH 7.4) supplemented with 1 mM DTT, 1 mM benzamidine, 0.5 mM sodium vanadate, and protease inhibitor cocktail (P8340; Sigma-Aldrich Canada, Oakville, ON, Canada) and then centrifuged 5 min at 1,000 *g* and 4°C. To immunoprecipitate eIF4E (23, 24), an aliquot of the supernatant was rotated overnight at 4°C with anti-eIF4E antibody. The antibody-antigen complex was collected by incubation for 1 h with Biomag goat anti-mouse IgG beads (no. 310004; Qiagen, Mississauga, ON, Canada), prewashed in 1% nonfat powdered milk in *buffer B* (20 mM Tris·HCl, pH 7.4, 150 mM NaCl, 5 mM EDTA, 0.1% 2-mercaptoethanol, 0.5% Triton X-100). The beads were recovered with a magnetic stand (Promega, Madison, WI) and were washed twice with *buffer B* and once with modified *buffer B* (50 mM Tris·HCl, 500 mM NaCl). Bound proteins were eluted by resuspending the beads in SDS-PAGE loading buffer followed by boiling for 5 min. The beads were collected by centrifugation, and the supernatants were stored at -80°C.

To quantify 4E-BP1, the eluates were separated by 15% SDS-PAGE. Proteins were then electrophoretically transferred to a polyvinylidene difluoride (PVDF) membrane (GE Healthcare Bio-Sciences, Baie d'Urfé, QC, Canada). Nonspecific sites were blocked by incubation in 5% milk powder in TBS-T (20 mM Tris, pH 7.6, 140 mM NaCl, 0.1% Tween 20) and then incubated overnight at 4°C with an anti-4E-BP1 polyclonal antibody (Bethyl Laboratories, Montgomery, TX). Membranes were washed and incubated in horseradish peroxidase (HRP)-conjugated goat anti-rabbit IgG (Bio-Rad Laboratories, Mississauga, ON, Canada). Signals were detected by enhanced chemiluminescence (ECL, GE Healthcare) using Chem DOC XRS Multi-Imager (Bio-Rad). Membranes were stripped (60°C incubation in 100 mM 2-mercaptoethanol, 2% SDS, 62.5 mM Tris·HCl, pH 6.7) and reblotted with anti-eIF4E polyclonal antibody.

An aliquot of the 1,000 *g* supernatant was separated by 10% (mTOR and S6K1) or 15% (S6 and Akt) SDS-PAGE, and proteins were transferred onto PVDF membranes. Membranes were probed with antibodies (Cell Signaling Technologies, New England Biolabs, Pickering, ON, Canada) that specifically detect phosphorylated mTOR (Ser 2448), S6K1 (Thr 389), Akt (Ser 473), and S6 (Ser 240/244, Ser 235/236). Incubation in secondary antibody and signal detection were as above with ECL or SuperSignal West Femto Maximum Sensitivity Substrate (Pierce Biotechnology, Rockford, IL). After detection, membranes were stripped to remove primary and secondary antibodies and then probed with antibodies to detect total mTOR, S6K1, Akt, and S6. Results are expressed as a fraction of phosphorylated to total protein. To detect phosphorylated 4E-BP1, supernatant was immediately centrifuged for 30 min at 10,000 *g* at 4°C. The supernatant was separated on 15% SDS-PAGE, and proteins were transferred to PVDF membranes and then probed with an anti-4E-BP1 antibody. Phosphorylated 4E-BP1 migrates with different mobilities. Results are expressed as the fraction of  $\gamma$  (the most phosphorylated) to the total of  $\alpha$ ,  $\beta$ , and  $\gamma$ .

Muscle RNA was isolated with the acid guanidinium thiocyanate-phenol-chloroform method (11). RNA was reverse transcribed with SuperScript III Reverse Transcriptase (Invitrogen Canada, Burlington, ON, Canada). The resulting cDNA was purified with the QIAquick PCR Purification Kit (Qiagen) and then used in quantitative PCR using the LightCycler FastStart DNA Master<sup>PLUS</sup> SYBR Green I and the LightCycler (Roche, Laval, QC, Canada). The following forward (F) and reverse (R) primers (5'-3') were used: ubiquitin F: GGC-AAGCAGCTGGAAGATGG, R: GAGCCAGTGACACCATCG; MAFbx F: ACCTCAGCAGTTACTGCAAC, R: GAAGGACATGCTGAATAGC; MuRF-1 F: ATCTTCCAGGCTGCAAAATC, R: GATCGTCACGGAGTGTAC. Each primer was designed to span

intron-exon junctions to ensure that genomic DNA would not be amplified. To correct for nonspecific effects of treatments on total mRNA, quantitative PCR was also carried out with porphobilinogen deaminase (PBGD) primers (F: GAAGTGGACCTGGTTGTTC; R: CCATCTGCAAACGGGAAAAC). Signals (crossover points) were converted to cDNA copies with standard curves conducted under identical run conditions. cDNA copies were expressed as a fraction of copies of PBGD cDNA.

An aliquot of 1,000 *g* supernatant was used to measure ubiquitinated protein levels. Equal amounts of proteins were separated by 10% SDS-PAGE and then transferred onto PVDF membranes. Immunoblotting was performed with a monoclonal anti-ubiquitin antibody (Santa Cruz Biotechnology, Santa Cruz, CA) followed by incubation in HRP-conjugated goat anti-mouse antibody (HRP-GAM, Bio-Rad). To correct for protein loading, membranes were stripped and blotted with a monoclonal anti  $\gamma$ -tubulin (Sigma-Aldrich Canada) antibody, followed by incubation in HRP-GAM. Signals were detected at both steps, and ubiquitin signals were expressed as a fraction of signals from the anti  $\gamma$ -tubulin blot.

*Statistical analyses.* Results are presented as means  $\pm$  SE. Subject characteristics and steady-state baseline and clamp hormone and substrate concentrations were compared between groups by independent *t*-tests. Responses to the clamp were analyzed with repeated-measures ANOVA (clamp as within-subject factor and type of protocol as between-subject factor). Differences in muscle translation initiation factors and gene expression between postabsorptive and Hyper-3 clamp periods were analyzed by paired *t*-test. Correlations were calculated with Pearson's correlation coefficient. Significance was set at 0.05. In light of a significant difference in the protein synthesis response with corresponding standard deviations from our previous studies, a minimum sample size of nine subjects per group was estimated, with power of 90% and  $\alpha$  of 0.05. Analyses were performed with SPSS 15.0 for Windows (SPSS, Chicago, IL).

## RESULTS

Anthropometric data (Table 1), serum lipids (normal, not shown), and metabolic and kinetic data in the basal state (Tables 2 and 3) were comparable between groups. Plasma AA concentrations (Table 4) in the Hyper-3 basal state were comparable to those of the isoaminoacidemic clamp in Hyper-1 subjects (8). The latter had established the suitability of TrophAmine for maintaining individual AA within their ranges of normal postabsorptive concentrations during the clamp.

Clamped plasma total BCAA, AA infusion rates, and totals infused in Hyper-3 were two- to threefold greater than in Hyper-1 (Table 2). The 25.7 g of AA infused in Hyper-3 would be the amount ingested in a 700-kcal meal with 15% of energy as protein, similar to our test meal. In contrast, maintaining hyperglycemia at 7.9 mmol/l in Hyper-3 required no greater glucose infusion rate than that to maintain euglycemia at 5.5 mmol/l in Hyper-1, because the increment in  $R_d$  was not greater. The total glucose infused was  $80 \pm 8$  g in Hyper-1 and  $79 \pm 6$  g in Hyper-3. Therefore, Hyper-3 glucose metabolic clearance was 40% less. This occurred despite 77% higher serum insulin, resulting in *M* values one-half those of the Hyper-1 clamp. The higher insulin was due to increased endogenous insulin secretion, as indicated by plasma C-peptide. Although C-peptide was measured in Hyper-1, absolute values were lower because of loss on storage. However, there was no increase during the clamp (not shown). The hyperglycemia and hyperaminoacidemia were likely responsible for the higher insulin and C-peptide. Glucagon did not decrease (perhaps

Table 2. Postabsorptive metabolic data and responses to Hyper-1 and Hyper-3 clamps

	Hyper-1		Hyper-3		ANOVA <i>P</i> Value Interaction
	Basal	Clamp	Basal	Clamp	
Plasma BCAA, $\mu\text{mol/l}$	404 $\pm$ 14	411 $\pm$ 13	382 $\pm$ 16	705 $\pm$ 20*	<0.001
Infusion rates					
Total amino acids, mg/min		49 $\pm$ 2		142 $\pm$ 9*	
Total amino acids infused, g		7.4 $\pm$ 0.4		25.7 $\pm$ 1.3*	
Plasma glucose, mmol/l	4.9 $\pm$ 0.1	5.5 $\pm$ 0.0	5.3 $\pm$ 0.1	7.9 $\pm$ 0.01*	<0.001
20% Glucose infusion rate, mg/min		560 $\pm$ 44		468 $\pm$ 35	
Glucose endogenous $R_a$ , mg/min	143 $\pm$ 5	-11 $\pm$ 4	153 $\pm$ 5	-4 $\pm$ 14	ns
Glucose $R_d$ , mg/min	142 $\pm$ 5	559 $\pm$ 44	155 $\pm$ 5	468 $\pm$ 35	ns
Glucose metabolic clearance rate, ml/min	160 $\pm$ 5	557 $\pm$ 41	163 $\pm$ 3	331 $\pm$ 23*	<0.001
M [ $R_d$ (mg/min)/insulin (pmol/l)]	2.86 $\pm$ 0.18	1.25 $\pm$ 0.10	2.59 $\pm$ 0.22	0.65 $\pm$ 0.10*	<0.001
Insulin, pmol/l	51 $\pm$ 2	450 $\pm$ 24	63 $\pm$ 5	798 $\pm$ 74*	<0.001
C-peptide, pmol/l	n/a	n/a	497 $\pm$ 59	2388 $\pm$ 244	
Glucagon, pmol/l	17.9 $\pm$ 1.50	13.0 $\pm$ 1.61	17.5 $\pm$ 1.51	14.8 $\pm$ 1.74	ns
Glucagon-to-insulin ratio	0.36 $\pm$ 0.04	0.03 $\pm$ 0.00	0.29 $\pm$ 0.04	0.02 $\pm$ 0.00	ns
Free fatty acids, $\mu\text{mol/l}$	441 $\pm$ 39	126 $\pm$ 11	362 $\pm$ 64	39 $\pm$ 6*	ns

Values are means  $\pm$  SE. BCAA, branched-chain amino acids;  $R_a$ , rate of appearance;  $R_d$ , rate of disappearance. M is calculated as glucose  $R_d$ /serum insulin concentration. \* $P$  < 0.001 vs. Hyper-1 clamp period, by independent *t*-test. A significant *P* value for the repeated-measures ANOVA means a difference in response from basal to clamp between the 2 protocols. ns, Not significant; n/a, data not available (see text).

because of the AA infusions); thus the fall in glucagon-to-insulin ratio was due to the rise in insulin. Endogenous glucose production was completely suppressed and serum FFA decreased markedly in both clamps.

The leucine kinetic responses (Table 3 and Fig. 1) to the Hyper-1 clamp included increased flux, decreased endogenous  $R_a$  (protein breakdown), increased nonoxidative  $R_d$  (synthesis), and reversal of the net balance (synthesis minus breakdown) from catabolism to anabolism, without altered oxidation. In contrast, in the Hyper-3 clamp, with the greater AA infusion rate (leucine exogenous  $R_a$  3-fold higher), total flux and synthesis increased more, oxidation tripled, and net balance doubled, but the difference in decrease in breakdown did not reach significance. Thus the increments in both synthesis and net synthesis were considerably greater in Hyper-3 ( $P$  < 0.001).

The plasma AA responses to the Hyper-3 clamp varied (Table 4). Concentrations for the 30 min before muscle biopsy and to the end of the infusions were maintained constant. There was no effect of the clamp on serine, glutamine, citrulline, or tyrosine, but a decrease in asparagine occurred. Leucine increased from 123  $\pm$  6  $\mu\text{mol/l}$  to 269  $\pm$  8  $\mu\text{mol/l}$  at 120 min and 274  $\pm$  9  $\mu\text{mol/l}$  at 180 min ( $P$  < 0.01). All other AA increased significantly, with greatest proportional increases in aspartate, methionine, isoleucine, and arginine and a small increase in alanine. Total essential AA increased 70% and total AA 36%. Of note is that the peak test meal concentrations

( $\mu\text{mol/l}$ ) of the following individual and grouped AA did not differ from those during Hyper-3: leucine, 261  $\pm$  9; isoleucine, 159  $\pm$  9; valine, 297  $\pm$  8; total essential, 1,541  $\pm$  73; and total AA, 3,632  $\pm$  215. In Hyper-1, the clamp total essential (945  $\pm$  20  $\mu\text{mol/l}$ ) and total (2,564  $\pm$  40  $\mu\text{mol/l}$ ) AA were identical to the basal Hyper-3 concentrations (939  $\pm$  29 and 2,467  $\pm$  87  $\mu\text{mol/l}$ , respectively).

The muscle analyses showed a marked increase in Akt phosphorylation (Fig. 2A) and changes in the components of protein synthetic and catabolic pathways, compared with the postabsorptive state: a trend toward increased phosphorylation of mTOR (Fig. 2B) and a significant increase in that of S6K1 (Fig. 3A) and 4E-BP1 (Fig. 4A), downstream substrates of mTOR, as well as of S6 ribosomal protein, substrate of S6K1 (Fig. 3B), were found. The amount of eIF4E bound to 4E-BP1 as an inactive complex was decreased (Fig. 4B). Expression of mRNAs of components of ubiquitin-dependent proteolysis (ubiquitin, ligases MAFbx/Atrogin-1 and MuRF-1) did not change (Fig. 5A). However, there was a significant reduction of ubiquitinated proteins ( $P$  < 0.01; Fig. 5B).

## DISCUSSION

Our novel Hyper-3 clamp simulates a fed steady state. The amounts of carbohydrate and protein infused over 3 h were comparable to those of our test meal that defined the

Table 3. Leucine kinetics during Hyper-1 and Hyper-3 clamps

	Hyper-1		Hyper-3	
	Basal	Clamp	Basal	Clamp
Total $R_a$ (flux)	140.4 $\pm$ 4.8	167.5 $\pm$ 7.1‡	138.0 $\pm$ 5.1	251.9 $\pm$ 9.3‡‡
Oxidation	33.6 $\pm$ 1.4	37.2 $\pm$ 1.7	27.0 $\pm$ 1.2	95.8 $\pm$ 5.1‡‡
Endogenous $R_a$ (breakdown)	140.4 $\pm$ 4.8	115.3 $\pm$ 6.3‡	138.0 $\pm$ 5.1	100.2 $\pm$ 6.7‡
Exogenous $R_a$ (infusion rate)		52.0 $\pm$ 1.6		151.7 $\pm$ 10.0‡
Nonoxidative $R_d$ (synthesis)	106.8 $\pm$ 3.5	130.3 $\pm$ 6.7‡	110.9 $\pm$ 4.1	156.2 $\pm$ 6.2*‡
Nonoxidative $R_d$ - endogenous $R_a$ (net balance)	-33.6 $\pm$ 1.4	15.0 $\pm$ 1.3‡	-27.0 $\pm$ 1.2	55.9 $\pm$ 6.2‡‡

Values (in  $\mu\text{mol/min}$ ) are means  $\pm$  SE. \* $P$  < 0.05, † $P$  < 0.001 vs. Hyper-1 clamp period, by independent *t*-tests. ‡ $P$  < 0.01 vs. corresponding basal values, by paired *t*-test.

Table 4. Plasma amino acid concentrations during Hyper-3 clamp

Amino Acids	Basal	Clamp 120 min	Clamp 180 min
Taurine	41 ± 3	51 ± 6*	48 ± 5*
Aspartate	8 ± 1	18 ± 1†	18 ± 1†
Asparagine‡	44 ± 2	30 ± 2†	25 ± 2*
Serine	77 ± 6	89 ± 9	88 ± 9
Glutamate	53 ± 2	68 ± 3†	69 ± 3†
Glutamine‡	544 ± 26	522 ± 39	507 ± 40
Glycine	219 ± 18	262 ± 27*	257 ± 27*
Alanine	271 ± 13	296 ± 16*	284 ± 15*
Citrulline‡	41 ± 3	40 ± 3	40 ± 3
Tyrosine	65 ± 2	61 ± 3	56 ± 3
Threonine	123 ± 7	153 ± 11†	149 ± 11†
Methionine	23 ± 1	58 ± 3†	59 ± 3†
Valine	205 ± 8	280 ± 8†	286 ± 9†
Isoleucine	55 ± 3	150 ± 7†	152 ± 7†
Leucine	123 ± 6	269 ± 8†	274 ± 9†
Phenylalanine	65 ± 1	110 ± 4†	110 ± 5†
Tryptophan	46 ± 2	73 ± 3†	73 ± 3†
Lysine	226 ± 16	391 ± 43†	390 ± 47†
Histidine	74 ± 2	124 ± 7†	122 ± 8†
Arginine	84 ± 2	206 ± 9†	210 ± 10†
Ornithine	83 ± 15	134 ± 25†	135 ± 25†
Total essential AA	939 ± 29	1,607 ± 79†	1,614 ± 85†
Total AA	2,467 ± 7	3,384 ± 196†	3,350 ± 206†

Values (in μmol/l) are means ± SE. AA, amino acids. \**P* < 0.05, †*P* < 0.01 vs. Basal; all AA remained constant between 120 and 180 min. ‡Not present in AA solution infused.

target clamp glycemia and aminoacidemia. The isotopic tracer/tracee steady states that were achieved (not shown) fulfill the prerequisite for the glucose and leucine kinetic methods used. In the Hyper-1 clamps the hyperinsulinemia approximated our test meal peak postprandial concentrations (~450 pmol/l). The insulin infusion rate was the

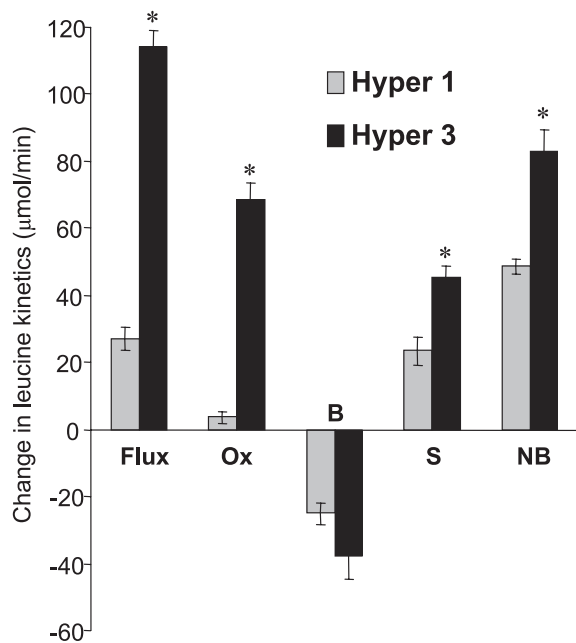


Fig. 1. Changes in whole body leucine kinetics (clamp minus basal) in response to the Hyper-3 clamp compared with the Hyper-1 clamp. OX, oxidation; B, breakdown; S, synthesis; NB, net balance. Values are means ± SE. \**P* < 0.001 vs. Hyper-1 by independent *t*-tests.

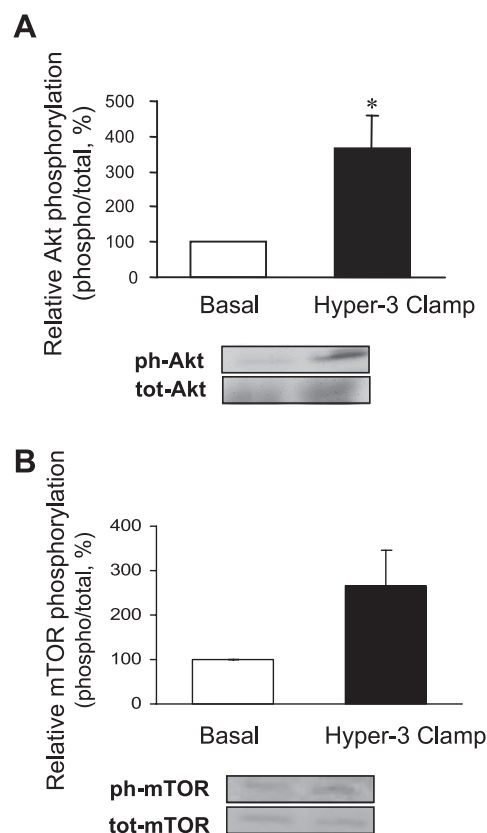


Fig. 2. Activation of Akt (A) and mammalian target of rapamycin (mTOR, B) in skeletal muscle after 2 h of hyperinsulinemia, hyperglycemia, and hyperaminoacidemia (Hyper-3 clamp) relative to the postabsorptive state (Basal). Data are expressed as phosphorylated (ph) Akt on serine 473 and mTOR on serine 2448 over total protein (tot), as % of basal. Representative Western blots are shown. \**P* < 0.05 vs. Basal.

standard used in studies of insulin resistance of glucose metabolism (13, 31) and used in our previous studies (7–10, 37). However, in the Hyper-3 clamp, because of the endogenous insulin response to hyperglycemia plus hyperaminoacidemia, serum levels were further elevated (~800 pmol/l). Insulin-mediated effects in the Hyper-3 clamp might thus be greater than in the Hyper-1 clamp, unless their maximal responses had already been achieved. This is the case for endogenous glucose production, which was totally suppressed, as reported previously (26). The absence of significant differences in suppression of whole body protein catabolism also demonstrates that the greater hyperinsulinemia was unable to decrease it further, consistent with absence of further suppression at >300 pmol/l (46). Likewise, the hyperaminoacidemia had no further suppressive effect.

The greater hyperinsulinemia in the absence of hyperaminoacidemia would have been expected to further increase glucose uptake, whose dose response has been shown to be half-maximal at 800 and maximal above 6,000 pmol/l (25, 26). Nevertheless, despite 77% higher insulin in Hyper-3 glucose *R<sub>d</sub>* was not significantly different. This indicates that physiological hyperaminoacidemia restrains the increase of insulin-mediated glucose uptake (14, 44), as does even greater hyperaminoacidemia (27, 47). Furthermore, hyperglycemic, hyperinsulinemic clamps (that would cause

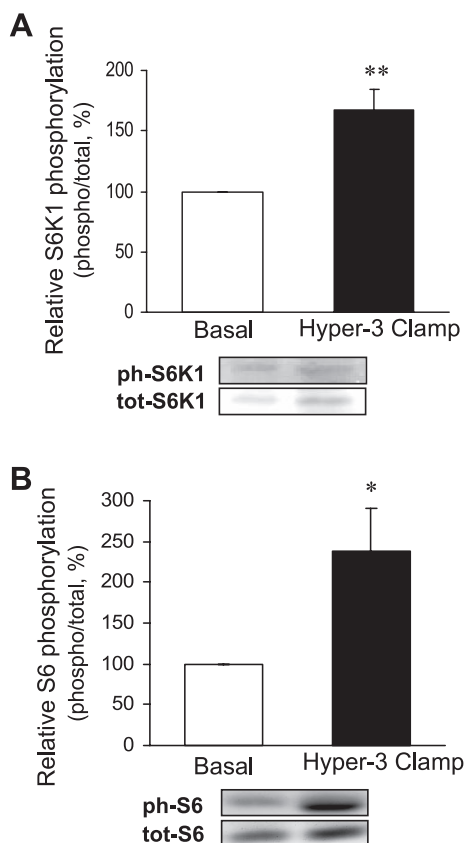


Fig. 3. Phosphorylation of S6K1 (threonine 389, *A*) and ribosomal S6 protein (serine 240/244 and serine 235/236, *B*) in skeletal muscle after 2 h of hyperinsulinemia, hyperglycemia, and hyperaminoacidemia (Hyper-3 clamp) relative to the postabsorptive state (Basal). Data are expressed as in Fig. 2. \* $P < 0.05$ , \*\* $P < 0.01$  vs. Basal.

hypoaminoacidemia) increase glucose  $R_d$  more than with euglycemia (32). In our study, at  $\sim 8$  mmol/l glycemia both metabolic clearance rate and  $M$  values were less than in the Hyper-1 clamp (Table 2). Furthermore, the lower FFA in Hyper-3 points to AA being responsible, because if there is an effect at this very low concentration it would be expected to be associated with greater insulin-mediated glucose uptake.

We are unaware of previous hyperinsulinemic clamp studies that combined clamped hyperglycemia with hyperaminoacidemia in normal subjects. In euglycemic somatostatin clamps with insulin at 430 pmol/l, lower muscle glucose uptake by the supraphysiological elevation of AA (vs. hypoaminoacidemia) was termed “insulin resistance” (27, 47). Although not always found, this effect has been reported previously (1, 42, 44). Our data are compatible with an alternative interpretation: rather than resistance to insulin, a physiological response to concurrent glucose and AA provision. Despite the greater hyperinsulinemia, our physiological hyperaminoacidemia was still remarkably effective at restraining the expected increment in glucose uptake. Although we cannot provide mechanistic insights into this effect, previous data suggest that overactivation of S6K1 is responsible for attenuating the insulin signaling of glucose metabolism by serine phosphorylation of insulin receptor substrate (IRS)-1 (36, 47).

The Hyper-3 leucine kinetic data (Table 3, Fig. 1) demonstrate 80% greater protein accretion than in the Hyper-1 clamp. This is probably attributable to the threefold greater leucine ( $\pm$  other AA) infusion, with a possible contribution from the higher insulin. Interestingly, the percent increase in serum total essential AA is the same as that in net balance. The positive leucine balance of  $56 \mu\text{mol}/\text{min}$  would be equivalent over 3 h to accretion of a maximum of 17 g of protein [assuming  $590 \mu\text{mol}$  leucine/g protein (49)], or 2/3 of the 25.7 g infused. If the fasting period of  $\sim 12$  h from the end of absorption of the evening meal until the beginning of the clamp had a constant net protein catabolic rate of  $27.0 \mu\text{mol}/\text{min}$  (Table 3), this could represent net catabolism of up to 32.9 g of protein. Therefore, the clamp conditions allowed for repletion of a substantial proportion of the protein lost overnight, further supporting the physiological relevance of this method. Considering the total glucose and AA infused over the 3 h in the two experiments, if the leucine oxidized is extrapolated to protein oxidized (29 vs. 11 g in Hyper-1), it could account for the 16-g-lower glucose uptake in Hyper-3. Although this is an overestimate, it still remains consistent with the restrained increment in glucose uptake in Hyper-3 being a physiological response to the availability of alternate energy substrate provided in excess of its maximal possible rate of incorporation

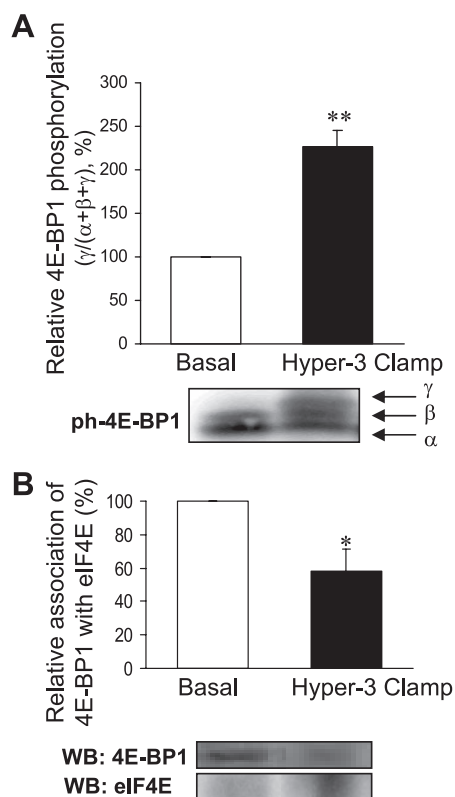


Fig. 4. Phosphorylation of 4E-binding protein 1 (4E-BP1; *A*) and association of eukaryotic initiation factor (eIF)4E with 4E-BP1 (*B*) in skeletal muscle after 2 h of hyperinsulinemia, hyperglycemia, and hyperaminoacidemia (Hyper-3 clamp) relative to the postabsorptive state (Basal). On phosphorylation, 4E-BP1 migrates with different mobilities ( $\alpha$ ,  $\beta$ , and  $\gamma$ , the  $\gamma$ -form being the most phosphorylated). Data are expressed as the fraction of 4E-BP1 in the  $\gamma$ -form to the total of all 4E-BP1 forms, as % of basal. Homogenates were subjected to immunoprecipitation followed by Western blotting (WB) to quantify 4E-BP1 associated with eIF4E. \* $P < 0.05$ , \*\* $P < 0.01$  vs. Basal.

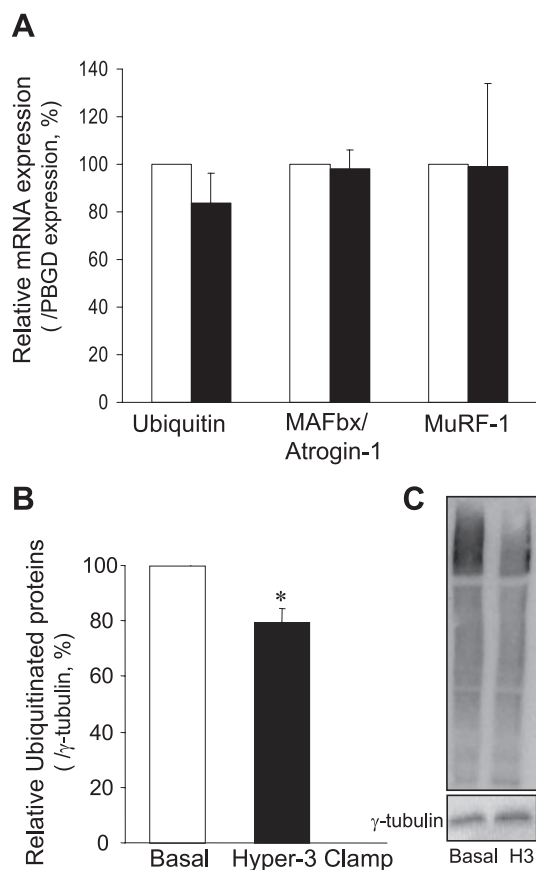


Fig. 5. mRNA expression of ubiquitin and ligases MAFbx/Atrogin-1 and MuRF-1, normalized for porphobilinogen deaminase (PBGD) (A) and total ubiquitinated proteins normalized for  $\gamma$ -tubulin (B) in skeletal muscle after 2 h of hyperinsulinemia, hyperglycemia, and hyperaminoacidemia (Hyper-3 clamp, filled bars) relative to the postabsorptive state (Basal, open bars). C: representative Western blot of ubiquitinated proteins. H3, Hyper-3 clamp. \* $P < 0.01$  vs. Basal.

into protein. The use of AA as fuel when supplied in excess of the requirement for protein synthesis has been reviewed (39). Further studies are required to distinguish between the metabolic states in which hyperaminoacidemia affects glucoregulation normally from those in which it causes insulin resistance.

Because muscle is a major contributor to whole body protein metabolism we determined whether changes at the molecular level in the muscle biopsies were consistent with those in whole body measurements. Akt activation by insulin affects both the synthetic and proteolytic pathways (40, 43). The Hyper-3 clamp increased phosphorylation of Akt, but that of mTOR did not reach statistical significance ( $P = 0.08$ ). However, increased phosphorylation downstream from mTORC1 occurred, of S6K1 and its substrate S6 ribosomal protein, as well as of 4E-BP1, accompanied by a reduction in inhibitory eIF4E·4E-BP1 complex. These changes are consistent with increased translation initiation and protein synthesis. Thus, although the possibility of mTORC1-independent activation cannot be excluded, the change in phosphorylation of the downstream targets without significant change in mTOR phosphorylation is more likely attributable to the variance of individual subject responses, and probably contributed to by its rapid and transient phosphorylation observed in other systems. Furthermore, mTORC1 activity is regulated by

binding of the substrate adaptor raptor, which may be of more physiological relevance than Ser 2448 phosphorylation of mTOR (35, 50).

We are unaware of published data on the fed-state regulation of molecular steps of muscle proteolysis in human subjects. Fasting in rodents increases mRNA levels of ubiquitin and the ubiquitin protein ligases MAFbx and MuRF-1 (28), and feeding suppresses them. Fasting also increases ubiquitinated protein levels (48). Since Akt activation suppresses MAFbx mRNA via phosphorylation of FOXO proteins, its suppression was likely too short for changes in gene expression to be observed, although we cannot exclude the possibility that expression of other proteases was modified. Our methodology is able to detect such suppression, because a marked decrease of MuRF-1 and MAFbx mRNA was observed in similar biopsies after intravenous glucose and AA were given perioperatively to patients undergoing abdominal surgery (41). The Hyper-3 clamp did suppress ubiquitinated protein levels by 20%, consistent with decreased ubiquitin-dependent proteolysis. Such reduction implies 1) decreases in the amount and/or activity of ligases that are independent of changes in transcription and/or 2) increases in the amount and/or activity of the deubiquitinating enzymes that remove ubiquitin from proteins (12). Ligases and deubiquitinating enzymes can be regulated by phosphorylation (20). It remains to be determined whether activated Akt or its effector phosphorylation through the insulin signaling cascade may regulate these enzymes by phosphorylation/dephosphorylation.

In conclusion, we have used a fed-state clamp to quantify *in vivo* responses and concurrently characterize the simultaneous regulation of molecular steps involved in protein synthetic and ubiquitin-dependent proteolytic pathways and have shown that these components respond to the fed state in the skeletal muscle. We previously demonstrated alterations in whole body protein metabolism in obesity, type 2 diabetes, and aging. This novel, physiologically relevant clamp, combined with muscle biopsies, will permit concurrent characterization of the synthetic and ubiquitin-proteasome contribution to catabolic mechanisms of insulin resistance of protein metabolism and of the interactions of protein with glucose metabolism in these states and identification of putative sites of defects.

#### ACKNOWLEDGMENTS

We thank Mary Shingler, Josie Plescia, Karen French, Marie Lamarche, Ginette Sabourin, Concettina Nardolillo, and Donato Brunetti for their assistance.

All authors contributed to the study design, analysis, and interpretation.

#### GRANTS

This work was supported by grants from the Canadian Institutes of Health Research to E. B. Marliss (MOP-62889) and S. S. Wing (MOP-82734) and from the National Institute of Diabetes and Digestive and Kidney Diseases to L. S. Jefferson (DK-15658) and salary awards to R. Gougeon from the McGill University Health Centre Research Institute and to S. Chevalier, J. A. Morais, and S. S. Wing from the "Fonds de recherche en santé du Québec."

## REFERENCES

1. **Abumrad NN, Robinson RP, Gooch BR, Lacy WW.** The effect of leucine infusion on substrate flux across the human forearm. *J Surg Res* 32: 453–463, 1982.
2. **Adegoke OAJ, Chevalier S, Labib N, Lamarche M, Gougeon R, Morais JA, Kimball SR, Jefferson LS, Wing SS, Marliss EB.** Whole-body protein turnover and molecular mechanisms regulating human skeletal muscle protein metabolism in the fed state (Abstract). *Diabetes* 55, Suppl 1: A289, 2006.
3. **Anthony JC, Reiter AK, Anthony TG, Crozier SJ, Lang CH, MacLean DA, Kimball SR, Jefferson LS.** Orally administered leucine enhances protein synthesis in skeletal muscle of diabetic rats in the absence of increases in 4E-BP1 or S6K1 phosphorylation. *Diabetes* 51: 928–936, 2002.
4. **Bolster DR, Vary TC, Kimball SR, Jefferson LS.** Leucine regulates translation initiation in rat skeletal muscle via enhanced eIF4G phosphorylation. *J Nutr* 134: 1704–1710, 2004.
5. **Bradley DC, Steil GM, Bergman RN.** Quantitation of measurement error with Optimal Segments: basis for adaptive time course smoothing. *Am J Physiol Endocrinol Metab* 264: E902–E911, 1993.
6. **Castellino P, Luzi L, Simonson DC, Haymond M, DeFronzo RA.** Effect of insulin and plasma amino acid concentrations on leucine metabolism in man. Role of substrate availability on estimates of whole body protein synthesis. *J Clin Invest* 80: 1784–1793, 1987.
7. **Chevalier S, Gougeon R, Choong N, Lamarche M, Morais JA.** Influence of adiposity in the blunted whole-body protein anabolic response to insulin with aging. *J Gerontol A Biol Sci Med Sci* 61: 156–164, 2006.
8. **Chevalier S, Gougeon R, Kreisman SH, Cassis C, Morais JA.** The hyperinsulinemic amino acid clamp increases whole-body protein synthesis in young subjects. *Metabolism* 53: 388–396, 2004.
9. **Chevalier S, Marliss EB, Morais JA, Lamarche M, Gougeon R.** The influence of sex on the protein anabolic response to insulin. *Metabolism* 54: 1529–1535, 2005.
10. **Chevalier S, Marliss EB, Morais JA, Lamarche M, Gougeon R.** Whole-body protein anabolic response is resistant to the action of insulin in obese women. *Am J Clin Nutr* 82: 355–365, 2005.
11. **Chomczynski P, Sacchi N.** Single-step method of RNA isolation by acid guanidinium thiocyanate-phenol-chloroform extraction. *Anal Biochem* 162: 156–159, 1987.
12. **Combaret L, Adegoke OA, Bedard N, Baracos V, Attaix D, Wing SS.** USP19 is a ubiquitin-specific protease regulated in rat skeletal muscle during catabolic states. *Am J Physiol Endocrinol Metab* 288: E693–E700, 2005.
13. **DeFronzo RA, Tobin JD, Andres R.** Glucose clamp technique: a method for quantifying insulin secretion and resistance. *Am J Physiol Endocrinol Metab Gastrointest Physiol* 237: E214–E223, 1979.
14. **Ferrannini E, Bevilacqua S, Lanzone L, Bonadonna R, Brandi L, Oleggini M, Boni C, Buzzigoli G, Ciociaro D, Luzi L, DeFronzo RA.** Metabolic interactions of amino acids and glucose in healthy humans. *Diabetes Nutr Metab* 3: 175–186, 1988.
15. **Finegood DT, Bergman RN, Vranic M.** Estimation of endogenous glucose production during hyperinsulinemic-euglycemic glucose clamps. Comparison of unlabeled and labeled exogenous glucose infusates. *Diabetes* 36: 914–924, 1987.
16. **Goran MI, Khaled MA.** Cross-validation of fat-free mass estimated from body density against bioelectrical resistance: effects of obesity and gender. *Obes Res* 3: 531–539, 1995.
17. **Gougeon R, Morais JA, Chevalier S, Pereira S, Lamarche M, Marliss EB.** Determinants of whole-body protein metabolism in subjects with and without type 2 diabetes. *Diabetes Care* 31: 128–133, 2008.
18. **Gougeon R, Pencharz PB, Sigal RJ.** Effect of glycemic control on the kinetics of whole-body protein metabolism in obese subjects with non-insulin-dependent diabetes mellitus during iso- and hypoenergetic feeding. *Am J Clin Nutr* 65: 861–870, 1997.
19. **Gougeon R, Styhler K, Morais JA, Jones PJ, Marliss EB.** Effects of oral hypoglycemic agents and diet on protein metabolism in type 2 diabetes. *Diabetes Care* 23: 1–8, 2000.
20. **Hunter T.** The age of crosstalk: phosphorylation, ubiquitination, and beyond. *Mol Cell* 28: 730–738, 2007.
21. **Jagoe RT, Goldberg AL.** What do we really know about the ubiquitin-proteasome pathway in muscle atrophy? *Curr Opin Clin Nutr Metab Care* 4: 183–190, 2001.
22. **Kimball SR, Jefferson LS.** Signaling pathways and molecular mechanisms through which branched-chain amino acids mediate translational control of protein synthesis. *J Nutr* 136: 227S–231S, 2006.
23. **Kimball SR, Jurasinski CV, Lawrence JC Jr, Jefferson LS.** Insulin stimulates protein synthesis in skeletal muscle by enhancing the association of eIF-4E and eIF-4G. *Am J Physiol Cell Physiol* 272: C754–C759, 1997.
24. **Kimball SR, Shantz LM, Horetsky RL, Jefferson LS.** Leucine regulates translation of specific mRNAs in L6 myoblasts through mTOR-mediated changes in availability of eIF4E and phosphorylation of ribosomal protein S6. *J Biol Chem* 274: 11647–11652, 1999.
25. **Kolterman OG, Insel J, Saekow M, Olefsky JM.** Mechanisms of insulin resistance in human obesity: evidence for receptor and postreceptor defects. *J Clin Invest* 65: 1272–1284, 1980.
26. **Kolterman OG, Scarlett JA, Olefsky JM.** Insulin resistance in non-insulin-dependent, type II diabetes mellitus. *Clin Endocrinol Metab* 11: 363–388, 1982.
27. **Krebs M, Krssak M, Bernroider E, Anderwald C, Brehm A, Meyerspeer M, Nowotny P, Roth E, Waldhausl W, Roden M.** Mechanism of amino acid-induced skeletal muscle insulin resistance in humans. *Diabetes* 51: 599–605, 2002.
28. **Lecker SH, Jagoe RT, Gilbert A, Gomes M, Baracos V, Bailey J, Price SR, Mitch WE, Goldberg AL.** Multiple types of skeletal muscle atrophy involve a common program of changes in gene expression. *FASEB J* 18: 39–51, 2004.
29. **Lecker SH, Solomon V, Mitch WE, Goldberg AL.** Muscle protein breakdown and the critical role of the ubiquitin-proteasome pathway in normal and disease states. *J Nutr* 129: 227S–237S, 1999.
30. **Leijssen DP, Elia M.** Recovery of  $^{13}\text{CO}_2$  and  $^{14}\text{CO}_2$  in human bicarbonate studies: a critical review with original data. *Clin Sci (Lond)* 91: 665–677, 1996.
31. **Luzi L, Petrides AS, De Fronzo RA.** Different sensitivity of glucose and amino acid metabolism to insulin in NIDDM. *Diabetes* 42: 1868–1877, 1993.
32. **Mandarino LJ, Consoli A, Jain A, Kelley DE.** Interaction of carbohydrate and fat fuels in human skeletal muscle: impact of obesity and NIDDM. *Am J Physiol Endocrinol Metab* 270: E463–E470, 1996.
33. **Matthews DE, Motil KJ, Rohrbach DK, Burke JF, Young VR, Bier DM.** Measurement of leucine metabolism in man from a primed, continuous infusion of L-[1- $^{13}\text{C}$ ]leucine. *Am J Physiol Endocrinol Metab* 238: E473–E479, 1980.
34. **Mitch WE, Goldberg AL.** Mechanisms of muscle wasting. The role of the ubiquitin-proteasome pathway. *N Engl J Med* 335: 1897–1905, 1996.
35. **Mothe-Satney I, Gautier N, Hinault C, Lawrence JC Jr, Van Obberghen E.** In rat hepatocytes glucagon increases mammalian target of rapamycin phosphorylation on serine 2448 but antagonizes the phosphorylation of its downstream targets induced by insulin and amino acids. *J Biol Chem* 279: 42628–42637, 2004.
36. **Patti ME, Brambilla E, Luzi L, Landaker EJ, Kahn CR.** Bidirectional modulation of insulin action by amino acids. *J Clin Invest* 101: 1519–1529, 1998.
37. **Pereira S, Marliss EB, Morais JA, Chevalier S, Gougeon R.** Insulin resistance of protein metabolism in type 2 diabetes. *Diabetes* 57: 56–63, 2008.
38. **Petrides AS, Luzi L, Reuben A, Riely C, DeFronzo RA.** Effect of insulin and plasma amino acid concentration on leucine metabolism in cirrhosis. *Hepatology* 14: 432–441, 1991.
39. **Rennie MJ, Bohe J, Smith K, Wackerhage H, Greenhaff P.** Branched-chain amino acids as fuels and anabolic signals in human muscle. *J Nutr* 136: 264S–268S, 2006.
40. **Sandri M, Sandri C, Gilbert A, Skurc C, Calabria E, Picard A, Walsh K, Schiaffino S, Lecker SH, Goldberg AL.** Foxo transcription factors induce the atrophy-related ubiquitin ligase atrogin-1 and cause skeletal muscle atrophy. *Cell* 117: 399–412, 2004.
41. **Schricker T, Meterissian S, Latterman R, Marliss EB, Adegoke OAJ, Mazza L, Eberhart L, Carli F, Nitschman E, Wykes LJ.** Avoidance of preoperative fasting by intravenous hypocaloric nutrition reduces whole body protein catabolism and stimulates albumin synthesis after surgery. *Ann Surg.* In press.

42. **Schwenk WF, Haymond MW.** Decreased uptake of glucose by human forearm during infusion of leucine, isoleucine, or threonine. *Diabetes* 36: 199–204, 1987.
43. **Stitt TN, Drujan D, Clarke BA, Panaro F, Timofeyva Y, Kline WO, Gonzalez M, Yancopoulos GD, Glass DJ.** The IGF-1/PI3K/Akt pathway prevents expression of muscle atrophy-induced ubiquitin ligases by inhibiting FOXO transcription factors. *Mol Cell* 14: 395–403, 2004.
44. **Tessari P, Inchiostro S, Biolo G, Duner E, Nosadini R, Tiengo A, Crepaldi G.** Hyperaminoacidaemia reduces insulin-mediated glucose disposal in healthy man. *Diabetologia* 28: 870–872, 1985.
45. **Tessari P, Nosadini R, Trevisan R, De Kreutzenberg SV, Inchiostro S, Duner E, Biolo G, Maressotti MC, Tiengo A, Crepaldi G.** Defective suppression by insulin of leucine-carbon appearance and oxidation in type 1, insulin-dependent diabetes mellitus. Evidence for insulin resistance involving glucose and amino acid metabolism. *J Clin Invest* 77: 1797–1804, 1986.
46. **Tessari P, Trevisan R, Inchiostro S, Biolo G, Nosadini R, De Kreutzenberg SV, Duner E, Tiengo A, Crepaldi G.** Dose-response curves of effects of insulin on leucine kinetics in humans. *Am J Physiol Endocrinol Metab* 251: E334–E342, 1986.
47. **Tremblay F, Krebs M, Dombrowski L, Brehm A, Bernroider E, Roth E, Nowotny P, Waldhausl W, Marette A, Roden M.** Overactivation of S6 kinase 1 as a cause of human insulin resistance during increased amino acid availability. *Diabetes* 54: 2674–2684, 2005.
48. **Wing SS, Haas AL, Goldberg AL.** Increase in ubiquitin-protein conjugates concomitant with the increase in proteolysis in rat skeletal muscle during starvation and atrophy denervation. *Biochem J* 307: 639–645, 1995.
49. **Wolfe RR.** *Radioactive and Stable Isotope Tracers in Biomedicine.* New York: Wiley-Liss, 1992, p. 388.
50. **Wullschlegel S, Loewith R, Hall MN.** TOR signaling in growth and metabolism. *Cell* 124: 471–484, 2006.

